AJNR

The cerebellum: 3. Anatomic-MR correlation in the coronal plane.

G A Press, J W Murakami, E Courchesne, M Grafe and J R Hesselink

AJNR Am J Neuroradiol 1990, 11 (1) 41-50
http://www.ajnr.org/content/11/1/41

The Cerebellum: 3. Anatomic-MR Correlation in the Coronal Plane

Gary A. Press[1]
James W. Murakami[2]
Eric Courchesne[2]
Marjorie Grafe[3]
John R. Hesselink[1]

Thin (5-mm) coronal high-field (1.5-T) MR images of four human brain specimens and 14 normal volunteers were correlated with myelin-stained microtomic sections of the specimen cerebella. The primary white-matter tracts innervating several hemispheric (posterior quadrangular, superior, and inferior semilunar, gracile, biventer, tonsil) and vermian (declive, folium, tuber) lobules are oriented perpendicularly to the coronal plane of section and are shown well on proton-density-weighted (long TR/short TE) and T2-weighted (long TR/long TE) spin-echo images, which provide excellent contrast between gray and white matter. Several of the surface sulci and fissures of the cerebellar hemispheres (including the superior posterior, horizontal, secondary, and posterolateral fissures) also course perpendicular to the coronal plane and are depicted well on T1-weighted (short TR/short TE) and T2-weighted images, which maximize contrast between CSF and parenchyma. The opportunity for side-to-side comparison of the hemispheres is a distinct advantage of the coronal view. Nevertheless, more obliquely oriented surfaces (preculminate, primary, inferior posterior, inferior anterior, and intrabiventral fissures) and deep hemispheric structures (primary white-matter tracts to central, anterior quadrangular, and floccular lobules) may be obscured by volume-averaging in the coronal plane; moreover, much of the finer anatomy of the vermis is depicted poorly. The constant surface and deep anatomy of the cerebellum revealed on coronal images in normal volunteers encourages detailed mapping.

MR imaging in the coronal plane should be especially useful in identifying, localizing, and quantifying normal and abnormal morphologic differences between the cerebellar hemispheres.

***AJNR* 11:41–50, January/February 1990; *AJR* 154: March 1990**

The cerebellum may be conceptualized as a stack of multiple transverse lobules, each of which is crescent-shaped with a wedgelike cross section that widens toward the periphery [1]. The spaces between the crescents are analogous to the cerebellar fissures. Transverse folds or sheets of white matter ("primary tracts" [1]) extend from central white-matter bodies (corpora medullaria) into the lobules. Because of this anatomic arrangement, it is most difficult to identify individual cerebellar lobules on axial MR images, which section parallel or nearly parallel to the courses of several important fissures and primary white-matter tracts. The sagittal plane of section (perpendicular to the courses of the fissures and white-matter tracts) proved ideal for the depiction of the anatomy of the lobules of the vermis and hemispheres, as described previously [1–3] (see Parts 1 and 2 of this report). The coronal plane of section (also perpendicular to the courses of many of the cerebellar fissures and white-matter tracts) offers an additional advantage by affording a side-to-side comparison on the same image.

This communication (Part 3) addresses specifically the topographic relationships of the cerebellar vermis and hemispheres in the coronal plane, and identifies detailed anatomy on coronal microtome and MR sections.

Received May 11, 1989; accepted July 18, 1989.

This work was supported by National Institute of Neurological Diseases and Stroke grant 5-RO1-NS19855 awarded to E. Courchesne.

[1] Department of Radiology and Magnetic Resonance Institute, University of California, San Diego, School of Medicine, 225 Dickinson St., San Diego, CA 92103-1990. Address reprint requests to G. A. Press.

[2] The Neuropsychology Research Laboratory, Children's Hospital Research Center, San Diego, CA 92123.

[3] Department of Pathology, University of California, San Diego, School of Medicine, San Diego, CA 92103-1990.

0195-6108/90/1101–041

Materials, Subjects, and Methods

MR studies of four formalin-fixed cadaver brains and 14 normal, healthy volunteers (13 male and one female 13–38 years old; mean age, 24.5 years) were performed in the coronal plane using a 1.5-T superconducting magnet (Signa, General Electric, Milwaukee). All volunteers and specimens were imaged with the use of a standard head coil. In all instances, 5-mm-thick slices with a matrix size of 256 × 256 were acquired using spin-echo sequences. A field of view (FOV) of 16–18 cm was used in volunteers; in specimen studies, an FOV of 12 cm was selected. T1-weighted sequences had the pulse parameters 600/20/4–6 (TR/TE/excitations). All volunteers received long TR examinations that were cardiac-gated to every other or every third heart beat, achieving an effective TR of approximately 2400–3800 msec, depending on the heart rate of each subject. Either two or four excitations per slice were used on long TR examinations of volunteers. A presaturation RF pulse for eliminating blood-flow artifacts along the Z axis (flow-void 1) was also used. Nongated long TR sequences performed on specimen brains had a TR of 2800 msec. TE values in long TR examinations were 20 and 70 msec, corresponding to proton-density-weighted and T2-weighted images, respectively. Slices obtained in volunteers were separated by a 3-mm gap. Specimen brains were imaged without interslice gaps (interleaved sections). A 28-sec scout sequence, 200/20/1 (24-cm FOV, 256 × 128 matrix), in the axial and sagittal planes was used to verify precise positioning of the subject or specimen brain before performing the protocol sequences. In every MR study, the coronal slices to be examined were selected by using this routine: On a midline sagittal scout image a line was drawn connecting the anterior aspect of the lingula and the nodulus [1]. Coronal sections through the entire cerebellum were then obtained parallel to the resulting line. The superior colliculus marked the anterior margin of the imaged region, whereas the inner table of the occipital bone at the level of the torcular Herophili marked the posterior margin in each instance.

Before MR, the specimen brains were fixed for 2–4 weeks in 10% neutral-buffered formalin. After MR, the cerebellum and brainstem were separated from the cerebral hemispheres and sectioned in the coronal plane at a thickness of 5 mm. The tissue blocks were dehydrated in a graded series of alcohols, cleared in xylene, and embedded in paraffin. Coronal sections of the cerebellum and brainstem were cut at a thickness of 15 μm using a Multirange Microtome (LKB, Stockholm). Adjacent anatomic sections corresponding closely to the MR images obtained by our normal volunteer protocol were stained with H and E and Luxol fast blue–cresyl violet.

The normal anatomic features of the cerebellar vermis and hemispheres visualized on the MR images and on the corresponding anatomic sections were determined by comparison with standard references of neuroanatomy [4, 5], myelin-stained cerebellar sections [6, 7], and cerebellar embryogenesis and development [8–11].

Many systems of nomenclature have been used to describe the normal anatomy of mammalian and human cerebella [6, 9, 10]. In this report we follow closely the terminologies chosen by Ito [9] and Larsell [10].

Results

Gross Anatomic Features of the Cerebellum

Prior reports have discussed in detail the gross anatomy of the vermis [2, 3] and the hemispheres [1] of the cerebellum. A brief review of key anatomic elements will help in understanding the appearance of the cerebellum on successive coronal sections and MR images shown in this article.

The two large lateral masses (hemispheres) and wormlike median segment (vermis) of the cerebellum are traversed by a series of fissures. The whole of the cerebellum is thereby divided into three lobes, each containing a number of transverse-oriented lobules (see Table 1). The arrangement of the fissures, lobes, and lobules of the cerebellum is shown diagrammatically in Figure 1. The deep primary fissure is an important landmark separating the anterior and posterior lobes of the cerebellum. The posterolateral fissure separates the flocculonodular lobe from the posterior lobe. Additional, shallower fissures subdivide the anterior and posterior lobes into lobules (I–IX of the vermis and HII–HIX of the hemispheres). No hemispheric counterpart of vermian lobule I exists in humans [6, 9]. The flocculonodular lobe of the cerebellum contains only one vermian lobule (nodulus [X]) and one hemispheric lobule (flocculus [HX]). With the exceptions of the prepyramidal fissure (confined to the vermis) and the inferior posterior and inferior anterior fissures (confined to the hemispheres), the remainder of the fissures extends across the entire cerebellum.

From a central confluence of white matter known as the corpus medullare, three paired cerebellar peduncles extend proximally into the brainstem, whereas smaller primary white-matter tracts radiate distally into the lobules of the vermis and hemispheres. The central body of white matter is much larger within the hemispheres than within the vermis [1, 6].

Situated within the medial aspect of the corpus medullare posterolateral to the fourth ventricle are the paired deep nuclei

TABLE 1: Components of the Human Cerebellum

Cerebellar Lobe	Vermian Lobule Nomenclature		Hemispheric Lobule Nomenclature	
	Ito [9]	Larsell [10]	Ito [9]	Larsell [10]
Anterior	Lingula	I	–	HI[a]
	Centralis	II, III	Central lobule	HII, HIII
	Culmen	IV, V	Quadrangular lobule, anterior portion	HIV, HV
Posterior	Declive	VI	Quadrangular lobule, posterior portion	HVI
	Folium vermis	Superior VIIA	Semilunar lobule, superior portion	HVIIA
	Tuber vermis	Inferior VIIA	Semilunar lobule, inferior portion	HVIIA
		VIIB	Gracile lobule	HVIIB
	Pyramis	VIIIA, VIIIB	Biventer	HVIII
	Uvula	IX	Tonsil	HIX
Flocculonodular	Nodulus	X	Flocculus	HX

Note.—This table is reprinted from Courchesne et al. [3].

[a] Hemispheric counterpart of vermian lobule I is usually absent in humans [6, 9].

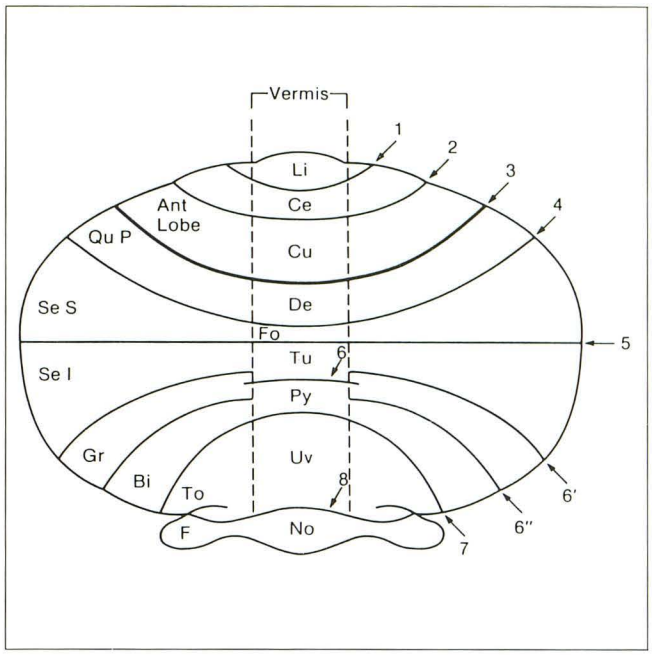

Fig. 1.—Diagram of lobar and lobular structure of cerebellum. This anatomic diagram of human cerebellum permits rapid identification of locus of any given term used in this article. Abbreviations used to designate the anterior lobe of the hemisphere as a whole, and each of the individual lobules of the posterior lobe of the hemisphere and flocculus, are positioned on the left side of the diagram. Arranged on the right side of the diagram are the numerals used to designate the major fissures subdividing the cerebellum. Confined by the central pair of broken lines are abbreviations used to designate the lobules of the vermis. Drawn in bold fashion is the primary fissure (3), which forms the boundary between the anterior and posterior lobes of the cerebellum. See key for abbreviations. (Reprinted from Press et al. [1].)

of the cerebellum. From medial to lateral they are the fastigial, globose, emboliform, and dentate nuclei. The largest and most familiar of the cerebellar nuclei, the dentate, has characteristic undulating outwardly convex margins [1].

Anatomic Features of the Cerebellum on Coronal Microtome and MR Sections

Analysis of the anatomic features of the cerebellum in six coronal sections showed sequential and reproducible changes in the contours and relationships of the individual lobules, corpora medullaria and smaller white-matter branches, brainstem, adjacent cisterns, and cerebellar fissures.

The individual lobules of the cerebellar *hemispheres* could be identified confidently and consistently by recognizing (1) the intrinsic order of branching and configuration of their primary white-matter tracts (evident on proton-density- and T2-weighted images) and (2) the sequence of fissures that divides the cerebellar parenchyma into discrete lobules (evident on T1- and T2-weighted images). The positions and configurations of the surrounding noncerebellar structures often provided helpful secondary clues. Within the *vermis*, however, identification of individual lobules on coronal sections was difficult because of volume-averaging of the more delicate fiber pathways and gray-matter structures, combined with variability of the precise angle of branching (and sectioning) of the primary tracts.

Key to Abbreviations Used in Figures

A	artifact of sectioning
Ant Lobe	anterior lobe of cerebellar hemisphere
ao	atlantooccipital joint
A Ve	lobules of anterior lobe of vermis
Bi	biventer
C	central lobule
Ce	centralis
Cm	corpus medullare
Cu	culmen
C1	posterior arch of C1 vertebra
D	dentate nucleus
De	declive
dm	digastric muscle
F	flocculus
fm	foramen magnum
Fo	folium vermis
Gr	gracile lobule
ibf	intrabiventral fissure
icp	inferior cerebellar peduncle
jb	jugular bulb
jt	jugular tubercle
Li	lingula
M	medulla
ma	rectus capitis posterior major muscle
mcp	middle cerebellar peduncle
Mi	midbrain
mi	rectus capitis posterior minor muscle
mv	medullary velum
No	nodulus
P	pons
pl	posterior cortical lip of foramen magnum
pt	primary white-matter tract
P Ve	lobules of posterior lobe of vermis
Py	pyramis
Qu A	quadrangular lobule, anterior portion
Qu P	quadrangular lobule, posterior portion
scp	superior cerebellar peduncle
Se I	semilunar lobule, inferior portion
Se S	semilunar lobule, superior portion
so	superior oblique muscle
tf	tranverse fossa
To	tonsil
Tu	tuber vermis
Uv	uvula
V	fourth ventricle
1	precentral fissure
2	preculminate fissure
3	primary fissure
4	superior posterior fissure
5	horizontal fissure
6	prepyramidal fissure (vermis only)
6′	inferior posterior fissure (hemisphere only)
6′′	inferior anterior fissure (hemisphere only)
7	secondary fissure
8	posterolateral fissure
9	vallecula
10	paramedian sulcus

Several observations can be made if the coronal anatomic or MR sections are considered in sequence from the most anterior plane (1) toward the most posterior plane (6).

Surface features:

1. In each coronal plane of section, the overall appearance of the brainstem and cerebellum is similar to a bird or butterfly with wings outstretched. In planes 1 and 2 (Figs. 2 and 3), the dorsal aspect of the midbrain, pons and/or fourth ventricle, and medulla constitute the "body" from which extend the "wings" formed by the middle cerebellar peduncles, corpora medullaria, and anterior portion of the hemispheric parenchyma. In planes 3–6 (Figs. 4–7), the body (now consisting of varying lobules of the vermis only) appears much smaller, whereas the wings (now consisting of the posterior portion of the hemispheric parenchyma and corpora medullaria or primary white-matter tracts) at first increase (plane 3, Fig. 4) and then decrease (planes 4–6, Figs. 5–7) in size.

2. The crescent-shaped lobules of the cerebellum have varying radii of curvature [1]; consequently, all are not present in every coronal section. For example, the group of anterior lobules (HII–HV) of the hemispheres and those of the vermis (I–V) have small radii relative to the posterior lobules (e.g., HVIIA and HVIIB); accordingly, the bulk of the anterior lobules is seen on the anterior-most three sections obtained by our MR protocol, whereas several posterior lobules are seen in five or six sections.

3. Unlike the crescent-shaped lobules forming the greater portion of the cerebellum, the flocculus and tonsil are smaller, ovoid lobules that protrude from the anterior and inferomedial surfaces of the hemispheres, respectively [1]. The flocculus is one of three bands of parenchyma adjacent to the middle cerebellar peduncle on coronal plane 1 (Fig. 2). The flocculus is sandwiched between a band of parenchyma above the peduncle (containing the anterior aspect of the central and

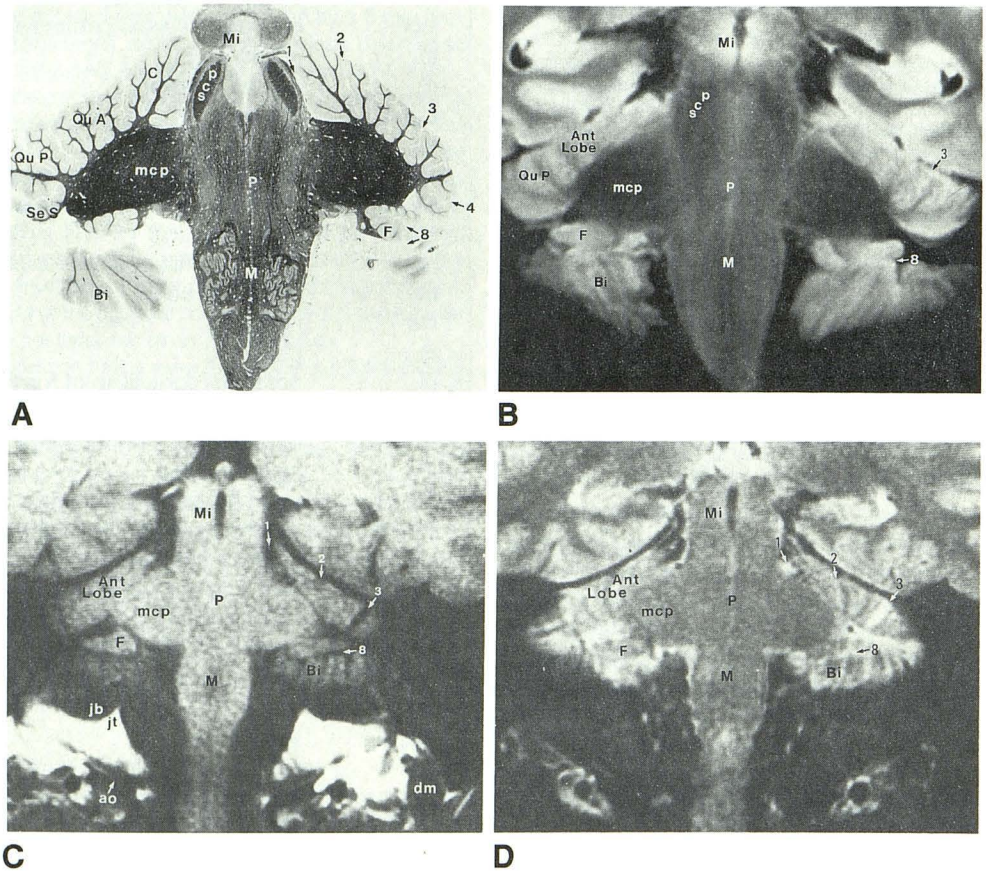

Fig. 2.—Plane 1, through brainstem, middle cerebellar peduncles, flocculus, and anterior-most portions of cerebellar hemispheres. See key for abbreviations.

***A*, Coronal microtome section of specimen brain. (Luxol fast blue–cresyl violet myelin stain)**

***B*, Corresponding coronal proton-density-weighted image, 2800/20/4, of the same specimen brain before sectioning.**

***C* and *D*, Coronal T1-weighted, 600/20/4 (*C*), and cardiac-gated T2-weighted, 3642/70/2 (*D*), images of 38-year-old normal male volunteer.**

Midbrain, pons, and medulla are continuous; middle cerebellar peduncles join pons to cerebellar hemispheres. Superior cerebellar peduncles diverge within midbrain just beneath their decussation. Three distinct symmetric bands of cerebellar parenchyma arranged above and below middle cerebellar peduncles appear to converge laterally in plane 1. Single band above peduncle represents anterior aspect of central and anterior quadrangular lobules on each side. Depending on precise angle of section and size of lobules, small portions of posterior quadrangular lobule and superior semilunar lobule may be sectioned at lateral-most aspect of this band. Middle band of tissue situated immediately beneath middle cerebellar peduncle represents flocculus of cerebellar hemisphere. Posterolateral fissure separates flocculus from third band of hemispheric tissue situated most inferiorly. This third band is the anterior aspect of the biventer. Primary white-matter tracts to anterior lobules of hemispheres, although shown well on thin (15-μm) microtome section (*A*), remain poorly resolved on thicker (5-mm) MR images (*B* and *D*) owing to volume-averaging. Extraparenchymal landmarks in this plane are best demonstrated on T1-weighted image (*C*) and include posterior aspect of jugular tubercle (jt), jugular bulb (jb), atlantooccipital joint (ao), and insertion of posterior belly of digastric muscle (dm) medial to mastoid tip.

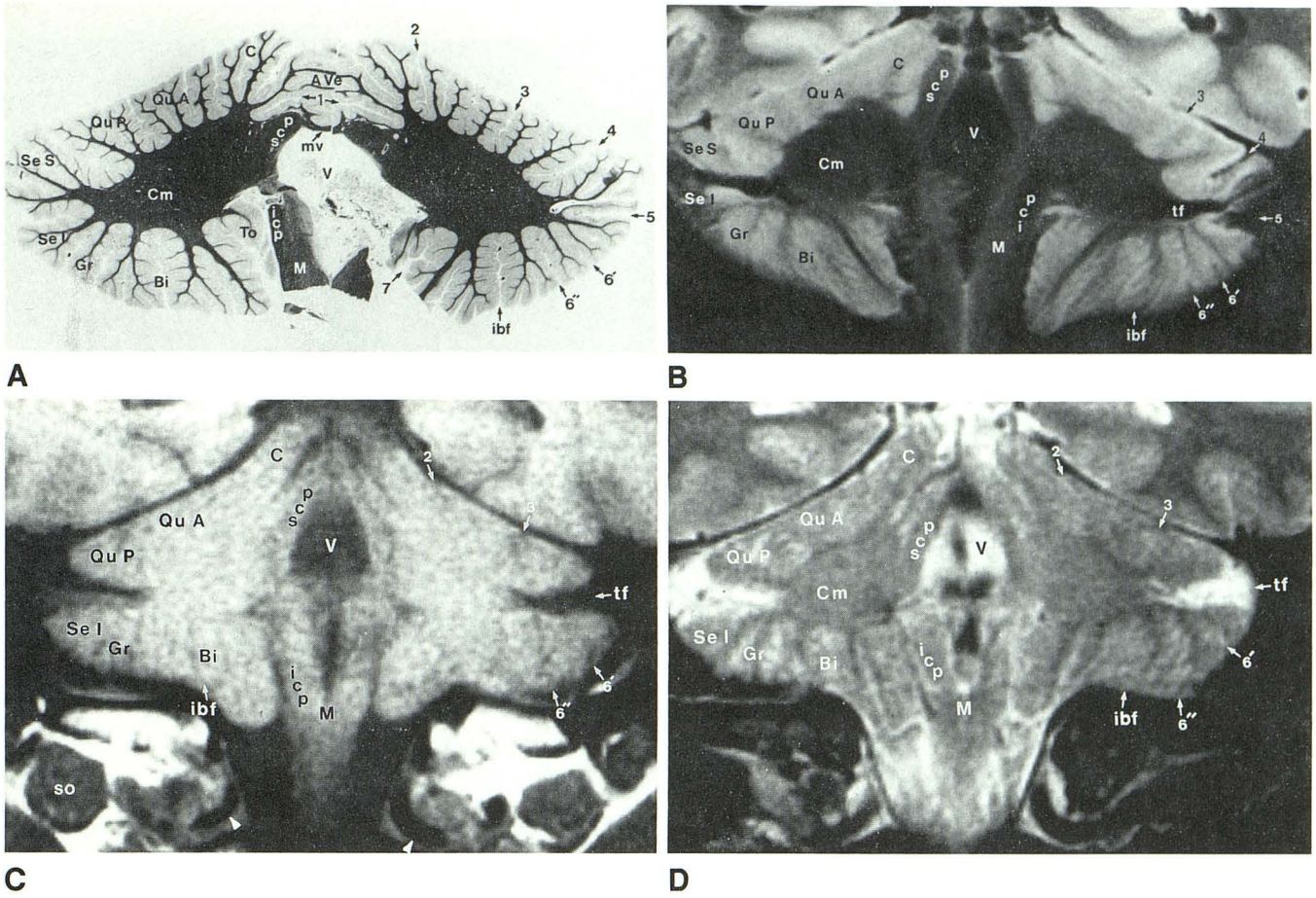

Fig. 3.—Plane 2, through fourth ventricle, superior and inferior cerebellar peduncles, medulla, corpora medullaria, and anterior and posterior lobes of cerebellum. See key for abbreviations.

***A*, Coronal microtome section of specimen brain. (Luxol fast blue–cresyl violet myelin stain)**

***B*, Corresponding coronal proton-density-weighted image, 2800/20, of same specimen brain before sectioning.**

***C* and *D*, Coronal T1-weighted, 600/20 (*C*), and cardiac-gated T2-weighted, 3642/70 (*D*), images of 38-year-old normal male volunteer.**

Flocculus is no longer present. Fourth ventricle is most prominent in this section. Its superolateral margins are formed by superior cerebellar peduncles; inferior cerebellar peduncles are separated from inferolateral margins of fourth ventricle by vestibular nuclei. In this section a laterally directed space, the transverse fossa (tf, *B–D*), is formed by converging folia of superior, lateral, and inferior hemispheric surfaces; this space may be distinguished from a true cerebellar fissure by its relatively large size and "nonanatomic" separation of lobules (e.g., posterior quadrangular and inferior semilunar lobules on *C* and *D*). Depending on precise plane of section, quadrigeminal plate or anterior extreme of anterior lobe of vermis may be sectioned above fourth ventricle. Primary white-matter tracts to larger lobules of posterior lobe of cerebellar hemispheres (e.g., inferior semilunar, gracile, biventer) are better resolved than those to smaller lobules of anterior lobe (*B* and *D*). This is true also of more posterior coronal MR images (compare with Figs. 4B, 4D, 5B, and 5D). On T1-weighted image (*C*), gray and white matter have similar signal intensity. Nevertheless, borders of parenchyma with surrounding CSF are better defined on T1-weighted image than on T2-weighted image (*D*), owing to persistent CSF flow artifacts adjacent to medulla, which resemble parenchyma on latter image. In this plane, note that biventer forms inferomedial border of each hemisphere, where it abuts medulla (*B* and *C*). Extraparenchymal landmarks identified in this plane in vivo include vertebral arteries (*arrowheads*) entering subarachnoid space above sulcus anteriosus and superior oblique muscles (so) sectioned transversely beneath occipital bone (C).

anterior quadrangular lobules) and an additional band below the peduncle (containing the anterior aspect of the biventer).

On coronal planes 3 and 4 (Figs. 4 and 5) (posterior to the medulla), the tonsils are seen in an immediately paramedian location, indenting the lateral aspects of the inferior vermis. The tonsils lie medial to the medial segment of the biventer on each side.

4. The superior posterior, horizontal, secondary, and posterolateral fissures, which form the boundaries of many of the cerebellar lobules, are reliably sectioned perpendicular to their course, and visible on coronal T1-weighted images (Figs. 2C, 3C, 4C, 5C, 6C, and 7C) or T2-weighted images (Figs. 2D, 3D, 4D, 5D, 6D, and 7D). The intracrural sulcus 1, which divides the superior semilunar lobule into superior and inferior portions [1, 6, 12], is also seen consistently on several of these images (Figs. 4C, 5C, 6C, and 7C). The lateral portion of the precentral fissure, which separates the central lobule from the junction of the midbrain and pons [1], is reliably seen on both the anatomic section (Fig. 2A) and MR images (Figs. 2C and 2D) through plane 1.

In normal volunteers, only the approximate locations of the more obliquely sectioned primary, inferior posterior, inferior anterior, and intrabiventral fissures may be identified on T2-weighted images (Figs. 3D, 4D, 5D, and 6D) as radially oriented peripheral zones of mild hyperintensity relative to parenchyma. The primary fissure lies in the zone of hyperintensity just medial and superior to the primary tract innervating the posterior quadrangular lobule; the inferior posterior fissure lies between the primary tracts innervating the inferior semilunar and gracile lobules; and the inferior anterior fissure

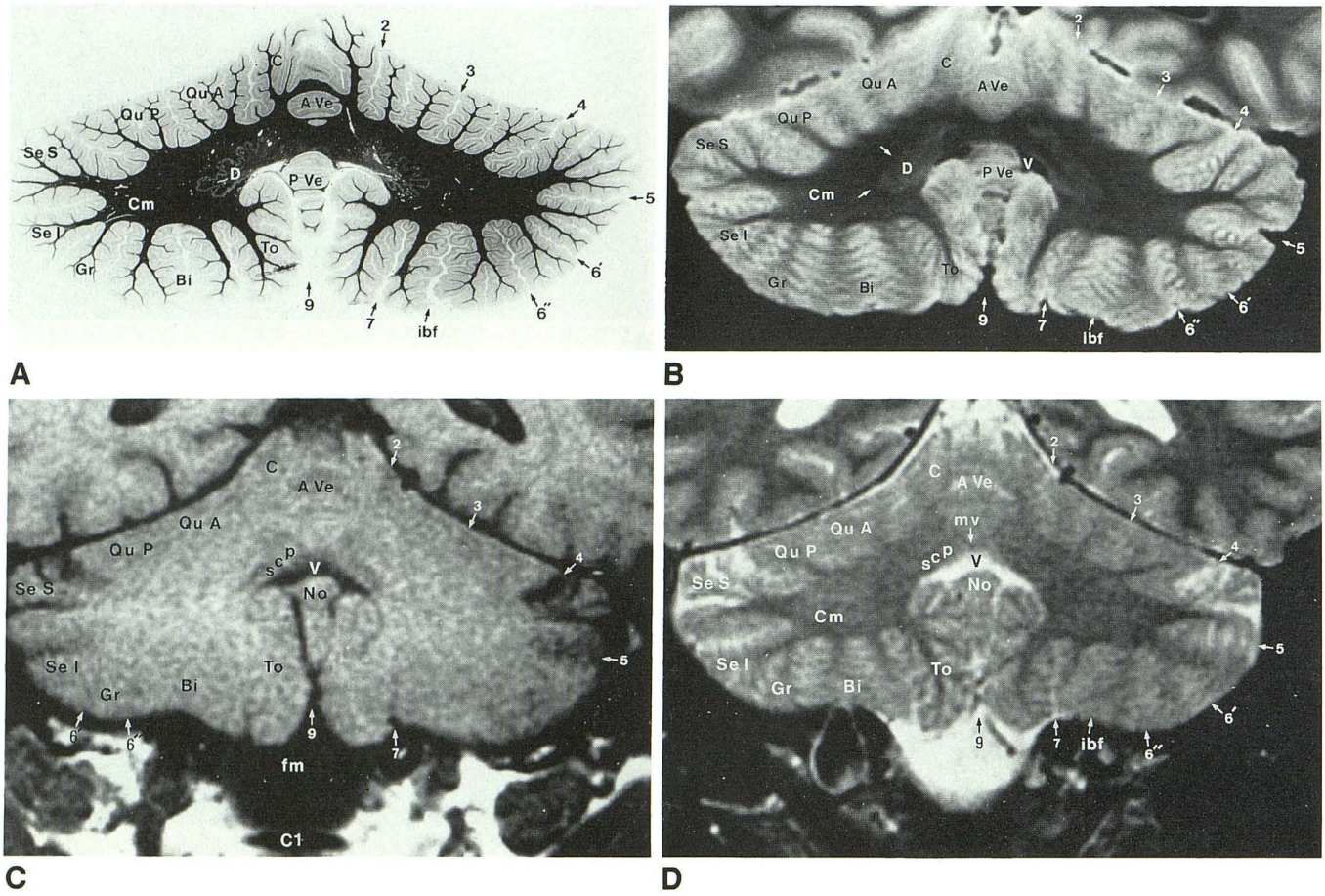

Fig. 4.—Plane 3, through anterior and posterior lobes of cerebellar hemispheres and vermis. See key for abbreviations.
***A*, Coronal microtome section of specimen brain. (Luxol fast blue–cresyl violet myelin stain)**
***B*, Corresponding coronal proton-density-weighted image, 2800/20, of same specimen brain before sectioning.**
***C and D*, Coronal T1-weighted, 600/20 (*C*), and cardiac-gated T2-weighted, 3642/70 (*D*), images of 38-year-old normal male volunteer.**
This is the initial section posterior to the medulla; only the posterolateral recesses of the fourth ventricle are included. The inferomedial aspect of each hemisphere is now formed by tonsils, which abut inferior aspect of vermis superiorly, and may abut each other inferiorly in midline. This is the final section to include a small portion of the central lobule. Corpus medullare attains its greatest size on this image. Dentate nucleus is seen clearly within medial aspect of each corpus medullare on proton-density-weighted image (*B*). White matter immediately peripheral to nucleus (*B, arrows*) has lower signal intensity than remainder of white matter, most likely because of iron deposition. Transverse fossa is no longer present. Horizontal fissure (5) separates superior and inferior semilunar lobules, whereas intracrural sulcus 1 (unlabeled) divides superior semilunar lobule into superior and inferior portions. Detailed anatomy of vermis is not well defined in coronal plane. Nevertheless, fourth ventricle, and overlying medullary velum and central confluence of vermian white matter, provide landmarks for dividing lobules of anterior lobe of vermis from those of posterior lobe and nodulus. Extraparenchymal landmarks in this plane include CSF within foramen magnum (fm, *C*) and vallecula posterior to brainstem, and posterior arch of C1 (C1, *C*).

lies between the primary tracts innervating the gracile lobule and the lateral segment of the biventer.

The preculminate fissure separating the central and anterior quadrangular lobules of the anterior lobe tends to be obscured completely on coronal MR images (Figs. 2B–2D, 3B–3D, and 4B–4D) relative to microtome sections (Figs. 2A, 3A, and 4A). The reasons for this are (1) its vertical orientation and small radius of curvature, which causes it to be sectioned most obliquely on coronal images, combined with (2) volume averaging inherent in 5-mm-thick MR sections. Thinner (15-μm) microtome sections minimize these difficulties and depict the finest anatomic details. The expected location of the preculminate fissure is indicated on the MR images (Figs. 2C, 2D, 3C, 3D, and 4B–4D).

Deep features:

1. In plane 1 (Fig. 2), the middle cerebellar peduncles join the pons to the corpora medullaria of the cerebellar hemispheres; the multiple slender primary tracts emanating directly from the periphery of the hemispheric corpora medullaria help to distinguish them from the middle cerebellar peduncles, which have no subordinate branches.

2. Unlike the larger middle cerebellar peduncles, which originate from the ventrolateral surface of each hemisphere and course nearly horizontally to reach the pons, the smaller superior and inferior cerebellar peduncles originate more medially and course nearly vertically to reach the brainstem. For this reason, the superior and inferior peduncles are sectioned longitudinally in the coronal plane, whereas the middle peduncles are sectioned more transversely. The fourth ventricle is the key to localizing the superior and inferior cerebellar peduncles in planes 2 and 3 (Figs. 3 and 4). The superior peduncles on each side and superior medullary velum in the midline form an arch over the top of the fourth ventricle (Figs. 3A and 4D); the inferior peduncles, on the other hand, lie

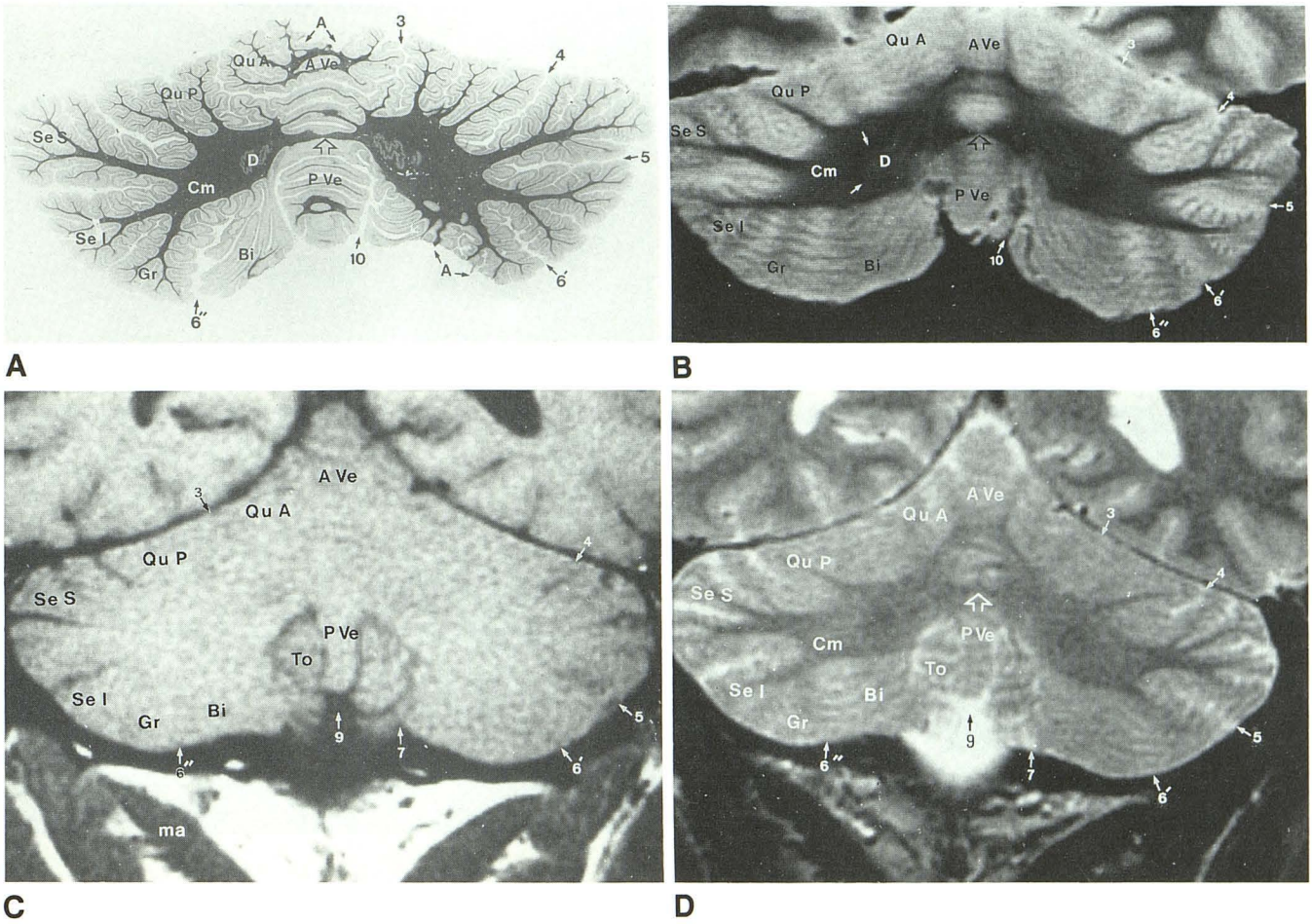

Fig. 5.—Plane 4, through anterior and posterior lobes of cerebellar hemispheres and vermis. See key for abbreviations.
***A*, Coronal microtome section of specimen brain. (Luxol fast blue–cresyl violet myelin stain)**
***B*, Corresponding coronal proton-density-weighted image, 2800/20, of same specimen brain before sectioning.**
***C* and *D*, Coronal T1-weighted, 600/20 (*C*), and cardiac-gated T2-weighted, 3642/70 (*D*), images of 38-year-old normal male volunteer.**
Corpora medullaria begin to decrease in size in this section. This is the last section to include a small portion of the tonsils (*C* and *D*). Two major bands of white matter crossing vermis are resolved on MR (*B* and *D*): superior band (unlabeled) is a portion of the primary tract to culmen that ascends in a nearly vertical course; inferior band (*open arrows*, *A*, *B*, and *D*) is horizontally oriented primary tract connecting to declive, folium, and tuber. These white-matter bands help distinguish anterior lobe of vermis (above upper band) from posterior lobe of vermis (below lower band) (*B* and *D*). Portion of vermis *between* two bands represents region of overlap between anterior and posterior lobes of vermis. *Solid arrows* indicate iron deposition in region of dentate. Distinctive V-shaped configuration of rectus capitus posterior major (ma) muscles is an extraparenchymal landmark identified in this plane (*C*).

medial to the corpora medullaria, separated from the fourth ventricle by the vestibular nuclei, and course inferiorly to form the greater part of the dorsal portion of the medulla (Fig. 3).

3. The branching pattern of the primary white-matter tracts to the hemispheres is constant [1], and many of the tracts may be identified in successive coronal sections. Above the primary fissure, only the single tract innervating the central lobule is frequently visualized on coronal MR planes 2 and 3 (Figs. 3B, 3D, 4B, and 4D). The tracts connecting to the anterior quadrangular lobule are sectioned more obliquely on coronal MR images and usually remain unresolved (Figs. 3B, 3D, 4B, 4D, 5B, and 5D). Nevertheless, they are well visualized on the anatomic sections (Fig. 3A, 4A, and 5A). The next clearly identifiable primary tracts on coronal MR connect the corpus medullare with the posterior quadrangular lobule. These tracts lie inferior to the primary fissure on planes 2–6 (Figs. 3–7). Situated immediately above and below the horizontal fissure are the primary tracts to the superior and inferior semilunar lobules, respectively; these tracts were seen in T2-weighted coronal MR planes 3–6 (Figs. 4–7) in all specimens and normal volunteers. The tract innervating the gracile lobule is resolved on three planes (Figs. 3–5) only, situated medial to the tract to the inferior semilunar lobule. The biventer receives two primary tracts, one directed inferolaterally and the other inferomedially to innervate the two segments of the lobule (planes 2 and 3, Figs. 3 and 4). The primary tract innervating the tonsil originates most medially from the inferior aspect of the corpus medullare. The tract may be identified only on coronal plane 3 (Fig. 4) immediately posterior to the brainstem.

4. Although, in our experience, the vermian white-matter branching pattern is constant also [3], only the horizontally oriented primary tract connecting with the declive, folium, and tuber [3] is sectioned reliably perpendicular to its course in

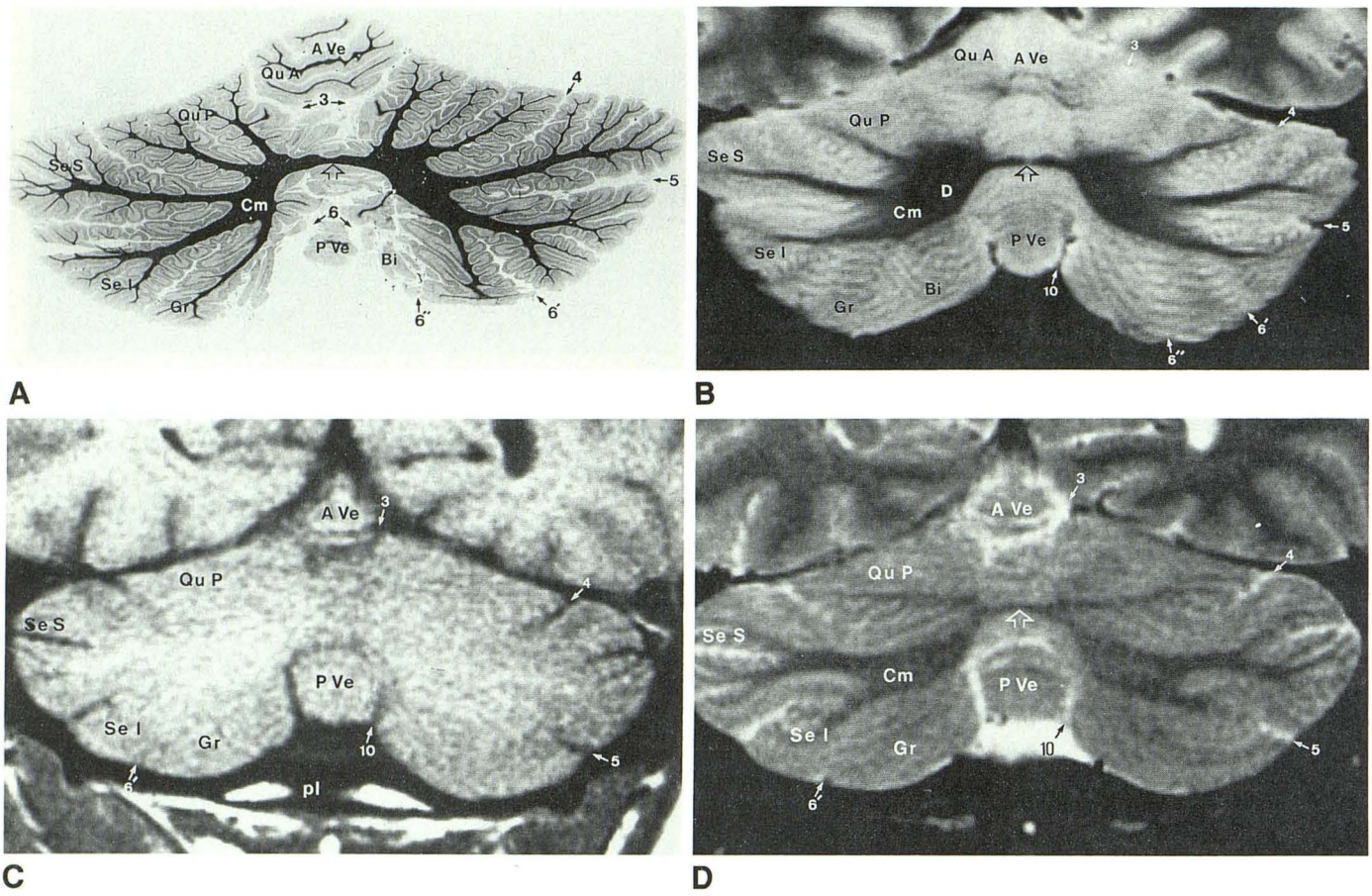

Fig. 6.—Plane 5, through posterior lobules of cerebellar hemispheres and anterior and posterior lobes of vermis. See key for abbreviations.
***A*, Coronal microtome section of specimen brain. (Luxol fast blue–cresyl violet myelin stain)**
***B*, Corresponding coronal proton-density-weighted image, 2800/20, of same specimen brain before sectioning.**
***C* and *D*, Coronal T1-weighted, 600/20 (*C*), and cardiac-gated T2-weighted, 3642/70 (*D*), images of 38-year-old normal male volunteer.**
This section includes mainly (if not exclusively) lobules of posterior lobe of hemispheres. Only a small portion of the anterior quadrangular lobule may be seen (*A* and *B*). Primary fissure (3, *A*, *C*, and *D*) traverses vermis above white-matter tract to declive, folium, and tuber (*open arrows*, *A*, *C*, and *D*), whereas prepyramidal fissure (6) may be identified beneath this tract and is especially well seen on anatomic section (*A*). Because this plane lies posterior to tonsils, it is the biventer or gracile lobule (depending on precise point of section) that forms inferomedial margin of cerebellar hemispheres. This is the final section to include a portion of the corpora medullaria. An extraparenchymal landmark identified in this plane in vivo is posterior lip (pl) of foramen magnum (*C*).

the coronal plane; this tract provides a helpful landmark for the localization of these three lobules as a group in MR planes 4–6 (Figs. 5–7). Less reliably visualized is the thicker, nearly vertically oriented primary tract innervating the culmen [3]; portions of this tract may be visualized in MR planes 4 and 5 (Figs. 5B, 5D, and 6B). The individual tracts to the lingula, centralis, pyramis, uvula, and nodulus of the vermis are indistinct on MR. The reasons for this include their oblique course relative to the coronal plane of section combined with their more delicate caliber, which permits volume-averaging with overlying gray matter on MR sections.

5. The dentate nucleus is visualized within the medial portion of each corpus medullare on planes 3 and 4 (Figs. 4 and 5); it appears as an oval curvilinear structure with an undulating margin. The dentate is seen best on proton-density-weighted images of specimen brains (Figs. 4B and 5B); its signal intensity is intermediate between that of white and gray matter. The white matter situated immediately peripheral to the nucleus is more hypointense than the remainder of the corpora medullaria (Figs. 4B and 5B). Deposition of iron within the region of the dentate nucleus and surrounding white matter [13] may account for these unique signal-intensity characteristics. The remaining deep nuclei (fastigial, globose, and emboliform) of the cerebellum, which lie within the corpora medullaria medial to the dentate, are not resolved on MR, likely owing to their small size (<1 cm) [1].

Imaging landmarks in coronal MR:

By using the slice-selection routine outlined in Materials, Subjects, and Methods, we obtained reproducible coronal sections through the cerebellum, posterior fossa, and posterior cervicocranial junction region in our normal volunteers. Nonparenchymal landmarks consistently identified in each of the six imaging planes in our volunteers included (1) plane 1 (Fig. 2C): posterior aspect of jugular tubercle, jugular bulb, atlantooccipital joint, and insertion of posterior belly of digastric muscle medial to mastoid tip; (2) plane 2 (Fig. 3C): vertical portion of sigmoid sinus, vertebral arteries entering subarachnoid space above sulcus arteriosus, and transverse section

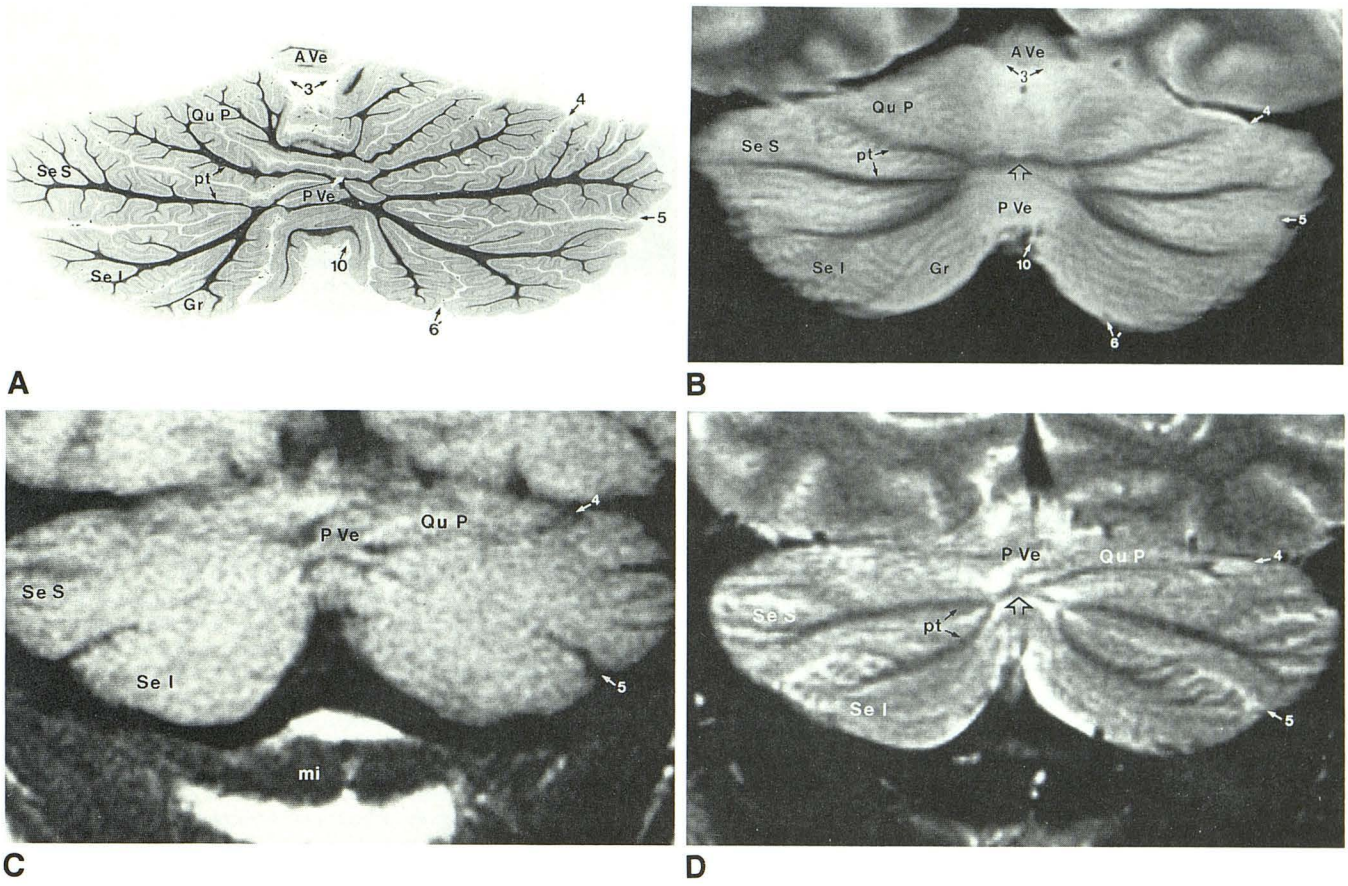

Fig. 7.—Plane 6, through posterior lobe of cerebellar hemispheres and vermis. See key for abbreviations.
***A*, Coronal microtome section of specimen brain. (Luxol fast blue–cresyl violet myelin stain)**
***B*, Corresponding coronal proton-density-weighted image, 2800/20, of same specimen brain before sectioning.**
***C* and *D*, Coronal T1-weighted, 600/20 (*C*), and cardiac-gated T2-weighted, 3642/70 (*D*), images of a 38-year-old normal male volunteer.**
Primary white-matter tracts innervating posterior quadrangular, superior, and inferior semilunar lobules on either side diverge laterally (*B* and *D*). Posterior extreme of vermis is sectioned in vicinity of termination of primary tract to declive, folium, and tuber (*open arrows*, *B* and *D*). Extraparenchymal landmark consistently identified in this plane in vivo is horizontally oriented junction of rectus capitis posterior minor (mi) muscles in midline immediately beneath occipital bone (*C*).

of superior oblique muscles beneath the occipital bone; (3) plane 3 (Fig. 4C): CSF within foramen magnum posterior to brainstem, and posterior arch of C1; (4) plane 4 (Fig. 5C): distinctive curve of the rectus capitis posterior major muscles diverging on either side of a triangular-shaped space filled with suboccipital fat; (5) plane 5 (Fig. 6C): posterior lip of foramen magnum; and (6) plane 6 (Fig. 7C): horizontal junction of the rectus capitus posterior minor muscles in the midline immediately beneath the occipital bone. The posterior aspect of the straight sinus at its junction with the torcular Herophili appears on the coronal section just posterior to the vermis (not shown).

Discussion

The surface features and deeper anatomy of the cerebellar vermis and hemispheres in normal individuals are highly standardized, encouraging detailed mapping and quantification. The overall transverse orientation of most of the lobules of the cerebellum explains why the sagittal and coronal planes of section are ideal for systematically depicting its physiologically significant parts. Excellent resolution of the horizontally oriented white-matter tracts, overlying cortex, surface sulci, and fissures of the bulk of the cerebellar hemispheres may be obtained by thin-section coronal MR. Moreover, the opportunity for side-to-side comparison is a distinct advantage provided by the coronal view. Nevertheless, those delicate primary tracts and surface features within the vermis and hemispheres that are oriented obliquely to the horizontal plane remain undisclosed by coronal MR owing to volume averaging. In particular, most of the detailed anatomy of the anterior lobe of the vermis and hemispheres and the inferior portion of the posterior lobe of the vermis (i.e., the pyramis, uvula, and nodulus) is poorly resolved on coronal images. Fortunately, the sagittal plane shows well the detailed anatomy of the entire vermis [2, 3] and the bulk of the hemispheres [1]. However, several primary tracts to the smaller lobules of the

anterior lobe of the cerebellar hemispheres remain unresolved even on 5-mm-thick sagittal MR images [1].

We speculated that the serpentine configuration of the dentate nuclei combined with iron deposition within their substance hampered their visualization on long TR sequences performed in the sagittal plane [1]. To our surprise, the dentate nuclei were visualized reliably in similarly fixed specimen brains studied in the coronal plane using the same sequences. Perhaps owing to their intrinsic shape, volume averaging of surrounding low-intensity white matter is decreased when the dentate nuclei are sectioned in the coronal plane. This result requires further investigation.

Knowledge of the detailed anatomy of the cerebellum as revealed by MR has proved useful in the comparison of various patient groups. For example, decreased size of the declive, folium, and tuber of the vermis was measured in a subpopulation of adult patients with autism [14]. A similar observation was made in patients with fragile X, a chromosomal abnormality associated with mental retardation and autisticlike symptoms [15], and in patients with schizophrenia associated with perinatal brain insult [16]. Recently, when the cumulative area of the cerebellar hemispheres of autistic individuals was measured on sagittal MR images, decreased cerebellar hemisphere size was demonstrated also [17].

Certain sensory, motor, and cognitive functions are known to be influenced predominantly by one or the other cerebellar hemisphere. For example, dysarthria is more common after injury to the left superior paravermian cerebellar hemisphere [18]; on the other hand, the inferolateral portion of the right hemisphere is important in semantic association, as shown by increased metabolic activity on positron emission tomographic scans [19]. In addition, naturally occurring asymmetries in cerebral-hemisphere (frontal-lobe) metabolism are correlated with asymmetry in the opposite direction in cerebellar-hemisphere metabolism in normal subjects [20]. Likewise, lesions of one cerebral hemisphere (frontal [21] or parietal [22] lobe) are associated with decreased glucose and oxygen metabolism and diminished blood flow in the contralateral cerebellar hemisphere (crossed cerebellar diaschisis). Most recently, evidence for a "reverse cerebellar diaschisis" (reduction in glucose metabolism within certain portions of the cerebral hemispheres owing to a reduction in specific cerebellar efferents to thalamus and forebrain structures) was found in patients with paraneoplastic cerebellar degeneration [23]. We speculate that MR imaging in the coronal plane will facilitate identification and quantification of normal and abnormal morphologic differences between the cerebellar hemispheres by allowing a side-to-side comparison in the same image. The detailed map of the cerebellum presented herein may enhance the specificity of studies correlating the anatomy of the cerebellum with its functions and metabolism.

Finally, we emphasize that the coronal and sagittal planes of section are ideal for visualizing intrinsic cerebellar anatomy. Accurate assessment of the normal anatomy of the brainstem [24], as well as localization and characterization of lesions of the posterior fossa extrinsic to the cerebellum (e.g., internal auditory canal neurinomas, meningiomas), may require axial images [25].

REFERENCES

1. Press GA, Murakami JW, Courchesne E, et al. The cerebellum in sagittal plane—anatomic-MR correlation: 2. The cerebellar hemispheres. *AJNR* **1989**;10:667–676, *AJR* **1989**;153:837–846
2. Press GA, Courchesne E, Murakami JW, Hesselink JR. The vermis in sagittal plane. Presented at the annual meeting of the American Society of Neuroradiology, Chicago, May **1988**
3. Courchesne E, Press GA, Murakami JW, et al. The cerebellum in sagittal plane—anatomic-MR correlation: 1. The vermis. *AJNR* **1989**;10:659–665, *AJR* **1989**;153:829–835
4. Nieuwenhuys R, Voogd J, Huijzen C. *The human central nervous system: a synopsis and atlas*, 2d ed. New York: Springer-Verlag, **1981**
5. Carpenter MB. *Human neuroanatomy*, 7th ed. Baltimore: Williams & Wilkins, **1976**
6. Angevine JB Jr, Mancall EL, Yakovlev PI. *The human cerebellum. An atlas of gross topography in serial sections*. Boston: Little, Brown, **1961**
7. DeArmond SJ, Fusco MM, Dewey MM. *Structure of the human brain: a photographic atlas*. New York: Oxford University, **1976**
8. Fox CA, Snider RS, eds. *The cerebellum*. Amsterdam: Elsevier, **1967**
9. Ito M. *The cerebellum and neural control*. New York: Raven, **1984**
10. Larsell O. The development of the cerebellum in man in relation to its comparative anatomy. *J Comp Neurol* **1947**;87:85–129
11. Lemire RJ, Loeser JD, Leech RW, Alvord EC Jr. *Normal and abnormal development of the human nervous system*. Hagerstown, MD: Harper & Row, **1975**
12. Larsell O, Jansen J. *The comparative anatomy and histology of the cerebellum*, vol. 3. *The human cerebellum, cerebellar connections and cerebellar cortex*. Minneapolis: University of Minnesota, **1972**
13. Drayer BP, Burger P, Darwin R, Riederer S, Herfkens R, Johnson GA. Magnetic resonance imaging of brain iron. *AJNR* **1986**;7:373–380
14. Courchesne E, Yeung-Courchesne R, Press GA, Hesselink JR, Jernigan TL. Hypoplasia of cerebellar vermal lobules VI and VII in infantile autism. *N Engl J Med* **1988**;318:1349–1354
15. Reiss AL, Patel S, Kumar AJ, Freund L. Preliminary communication: neuroanatomical variations of the posterior fossa in men with the fragile X (Martin-Bell) syndrome. *Am J Med Genet* **1988**;31:407–414
16. Nasrallah HA, Schwartzkopf SB, Coffman JA, Olson SC. Hypoplasia of the cerebellar vermal lobules VI and VII on MRI scans in schizophrenia is associated with perinatal brain insult (abstr). Presented at the International Congress of Schizophrenia Research, San Diego, April **1989**
17. Murakami JW, Courchesne E, Press GA, Yeung-Courchesne R, Hesselink JR. Reduced cerebellar hemisphere size and its relationship to vermal hypoplasia in autism. *Ann Neurol* **1989**;46:689–694
18. Lechtenberg R, Gilman S. Speech disorders in cerebellar disease. *Ann Neurol* **1978**;3:285–290
19. Petersen SE, Fox PT, Posner MI, Mintun MA, Raichle ME. Positron emission tomographic studies of the processing of single words. *Neuroscience* **1989**;1:153–170
20. Junck L, Gilman S, Rothley JR, Betley AT, Koeppe RA, Hichwa RD. A relationship between metabolism in frontal lobes and cerebellum in normal subjects studied with PET. *J Cognitive Neuropsykhol* **1988**;8:774–782
21. Martin WR, Raichle ME. Cerebellar blood flow and metabolism in cerebral hemisphere infarction. *Ann Neurol* **1983**;14:168–176
22. Lenzi GL, Frackowiak SJ, Jones T. Cerebral oxygen metabolism and blood flow in human cerebral ischemic infarction. *J Cereb Blood Flow Metab* **1982**;2:321–335.
23. Anderson NE, Posner JB, Sidtis JJ, et al. The metabolic anatomy of paraneoplastic cerebellar degeneration. *Ann Neurol* **1988**;23:533–540
24. Han JS, Bonstelle CT, Kaufman B, et al. Magnetic resonance imaging in the evaluation of the brainstem. *Radiology* **1984**;150:705–712
25. Press GA, Hesselink JR. MR imaging of cerebellopontine angle and internal auditory canal lesions at 1.5 T. *AJNR* **1988**;9:241–251